Numerical Methods and the Dampened, Driven Pendulum

Matthew Epland
Department of Physics, Duke University
(Dated: July 26, 2016)

The behavior of a dampened, driven simple pendulum was investigated numerically via the Euler–Cromer $\mathcal{O}\big((\Delta t)^2\big)$ and Rung–Kutta methods $\mathcal{O}\big((\Delta t)^4\big)$. The pendulum's resonance curves, nonlinear behavior, and chaotic properties were studied for a variety of driving frequencies, amplitudes, and initial conditions. Adapted from an assignment completed for PHYS 566 Computational Physics with Professor Bass.

I. INTRODUCTION

Damped, driven pendulums are a rich second order system for study, exhibiting many interesting behaviors such as resonance, nonlinear equations, and chaos. Furthermore they are a good system to model computationally as analytical solutions can be derived for comparison, in the limit of the linear, small angle approximation. Here a damped, driven simple pendulum was simulated with the Euler–Cromer and Rung–Kutta methods. By varying parameters of the system resonance, nonlinear effects and chaos were studied in turn, as well as the differences between the two simulation methods themselves.

II. THEORY

The equation of motion of a damped, driven pendulum (1) for small angles[1] is a second order linear equation. As written all of the constants are positive real numbers. It is helpful to rewrite (1) as (2) where $\omega_0^2 = g/l$ and $F(t)$ is the external driving force.

$$\frac{d^2\theta}{dt^2} = -\frac{g}{l}\theta - 2\gamma\frac{d\theta}{dt} + \alpha_D \sin(\Omega_D t) \tag{1}$$

$$\begin{aligned} \ddot{\theta} + 2\gamma\dot{\theta} + \omega_0^2\theta &= F(t) \\ F(t) &= \alpha_D \sin(\Omega_D t) \end{aligned} \tag{2}$$

The solution to (2) can be broken into two parts, the solution of the associated homogeneous equation where $F(t) = 0$, and any particular solution of (2). To begin with we will solve the homogeneous equation by assuming a solution of the form $\theta(t) \sim e^{rt}$, which is indeed a solution provided that r is a root of the characteristic equation (3). Using the quadratic formula we find the two roots to be $r_\pm$ (4), thereby specifying the homogeneous solution[2] (5).

$$r^2 + 2\gamma r + \omega_0^2 = 0 \tag{3}$$

$$r_\pm = -\gamma \pm \sqrt{\gamma^2 - \omega_0^2} \tag{4}$$

$$\theta(t)_{\text{Homogeneous}} = \begin{cases} Ae^{r_+ t} + Be^{r_- t} & \text{if } \gamma \neq \omega_0 \\ (A + Bt)\, e^{-\gamma t} & \text{if } \gamma = \omega_0 \end{cases} \tag{5}$$

It is easy to see from (4) that $\mathrm{Re}(r_\pm) < 0$ for all γ and ω_0, therefore the homogeneous solution (5) always decays away to nothing; it is a transient solution[3]. As we are primary interested in the steady state behavior of the pendulum we therefore need only be concerned with the particular solution from here on out.

---

[1] Where $\sin(\theta) \approx \theta + \mathcal{O}(\theta^2)$

[2] If $\gamma = \omega_0$, and therefore $r_+ = r_-$, we need to include a multiplicative factor of t on one of the solutions so that they are linearly independent.

[3] The homogeneous solutions importance in this case lies in it's ability to match the initial conditions of the pendulum, regardless of what the driving force is doing. For our pendulum the initial conditions are $\theta(t=0) = \theta_0,\ \omega(t=0) = 0$

We can find a particular, or steady state, solution (6) that works by trial and error. Plugging (6) into (2) with $F(t) = \alpha_D \sin(\Omega_D t)$ results in (7).

$$\theta(t)_{\text{Particular}} = \theta_P \sin(\Omega_D t - \phi) \tag{6}$$

$$\frac{\alpha_D}{\theta_P} \sin(\Omega_D t) = \left(\omega_0^2 - \Omega_D^2\right) \sin(\Omega_D t - \phi) + 2\gamma\Omega_D \cos(\Omega_D t - \phi) \tag{7}$$

While (7) may look rather messy, it is possible to extract the steady state amplitude $\theta_P(\Omega_D)$ and phase $\phi(\Omega_D)$. One of the simpler, but less rigorous[4], ways to do so is by making use of the trigonometric identity (8) with $\alpha = \Omega_D t - \phi$ and $\beta = \phi$. Rearranging (7) into (9), we can identify (10) term by term.

$$\sin(\alpha + \beta) = \sin(\alpha)\cos(\beta) + \cos(\alpha)\sin(\beta) \tag{8}$$

$$\sin(\alpha + \beta) = \sin(\alpha)\left(\frac{\theta_P}{\alpha_D}\left(\omega_0^2 - \Omega_D^2\right)\right) + \cos(\alpha)\left(\frac{2\gamma\Omega_D\theta_P}{\alpha_D}\right) \tag{9}$$

$$\cos(\phi) = \frac{\theta_P}{\alpha_D}\left(\omega_0^2 - \Omega_D^2\right) \qquad \sin(\phi) = \frac{2\gamma\Omega_D\theta_P}{\alpha_D} \tag{10}$$

Now that $\sin(\phi)$ and $\cos(\phi)$ are known, $\theta_P(\Omega_D)$ and $\phi(\Omega_D)$ (11 and 12) can be found from the sum of their squares and their ratio, respectively.

$$\theta_P(\Omega_D) = \frac{\alpha_D}{\sqrt{\left(\omega_0^2 - \Omega_D^2\right)^2 + 4\gamma^2\Omega_D^2}} \tag{11}$$

$$\phi(\Omega_D) = \arctan\left(\frac{2\gamma\Omega_D}{\omega_0^2 - \Omega_D^2}\right) \tag{12}$$

A. Resonance

As our pendulum is a driven oscillator we can expect it to exhibit resonant behavior at some driving frequency, Ω_{Res}. To find Ω_{Res} analytically we can employ the usual maximization method[5] of solving for where the first derivative is zero (13).

$$0 = \left.\frac{d\theta_P}{d\Omega_D}\right|_{\Omega_D = \Omega_{\text{Res}}} = -\frac{\alpha_D}{2}\left(\left(\omega_0^2 - \Omega_{\text{Res}}^2\right)^2 + 4\gamma^2\Omega_{\text{Res}}^2\right)^{-3/2}\left(-4\left(\omega_0^2 - \Omega_{\text{Res}}^2\right)\Omega_{\text{Res}} + 8\gamma^2\Omega_{\text{Res}}\right) \tag{13}$$

$$\Omega_{\text{Res}} = \sqrt{\omega_0^2 - 2\gamma^2} \tag{14}$$

Lastly, note that Ω_{Res} of (14) solves (13) when $\omega_0 \neq \gamma$. If $\omega_0 \approx \gamma$ the $(\cdots)^{-3/2}$ term diverges and we would need to set $\gamma = \omega_0$ at the beginning of the problem and redo the derivation. Here we choose $\omega_0 = 1.0\ s^{-1} \neq \gamma = 0.25\ s^{-1} \rightarrow \Omega_{\text{Res}} = 0.93541$ [rad/s], so this is not an issue.

---

[4] Since α and β are clearly correlated via their shared ϕ dependence, the term by term identification argument is somewhat suspect.
[5] Of course the resulting extrema could be a minimum of $\theta_P(\Omega_D)$, but in this case it is indeed a maximum as later figures show.

B. Euler–Cromer

The default Euler method is a simple technique for solving differential equations numerically, however its solutions usually do not conserve energy but tend to increase in total energy over time. We can remedy this by switching to the Euler–Cromer method, also known as the semi-implicit Euler method[6], by modifying the Euler method to use ω_{n+1} instead of ω_n when computing θ_{n+1}, see (15, 16).

$$\frac{d\theta}{dt} = f\left(t, \theta;\ \omega\right) \qquad \frac{d\omega}{dt} = \frac{d^2\theta}{dt^2} = g\left(t, \omega;\ \theta\right) \tag{15}$$

$$\theta_{n+1} = \theta_n + f\left(t_n, \theta_n;\ \underline{\omega_{n+1}}\right)\Delta t \qquad \omega_{n+1} = \omega_n + g\left(t_n, \omega_n;\ \theta_n\right)\Delta t \tag{16}$$

$$t_n = t_0 + n\Delta t = n\Delta t \tag{17}$$

For our pendulum we have:

$$f\left(t, \theta;\ \omega\right) = \omega \qquad g\left(t, \omega;\ \theta\right) = -\omega_0^2\theta - 2\gamma\omega + \alpha_D \sin\left(\Omega_D t\right) \tag{18}$$

C. Runge–Kutta

The Euler and Euler–Cromer methods work by sampling the differential equation once at the beginning of each time step, which when worked out gives them a final error of $\mathcal{O}\big(\left(\Delta t\right)^2\big)$. As such, an easy way to improve on the Euler method is to sample the differential equation more than once per time step. The family of numerical solutions of this type are called Runge–Kutta methods, of which the Euler method is the simplest member. In addition to the Euler–Cromer method we will be using *The* Runge–Kutta method, or RK4, which samples the differential equation four times per time step. The four samples are used in a weighted average in place of $f\left(t\right)$ and $g\left(t\right)$ in the Euler method, compare (15, 16) to (19, 20). By averaging over four samples per time step the RK4 method decreases the error to $\mathcal{O}\big(\left(\Delta t\right)^4\big)$, quite a nice improvement for relatively little effort.[7] For our pendulum $f\left(t\right)$ and $g\left(t\right)$ remain the same as before (18).

$$\theta_{n+1} = \theta_n + \frac{1}{6}\left(k_1 + 2k_2 + 2k_3 + k_4\right)\Delta t \qquad \omega_{n+1} = \omega_n + \frac{1}{6}\left(l_1 + 2l_2 + 2l_3 + l_4\right)\Delta t \tag{19}$$

$$\begin{aligned}
k_1 &= f\left(t_n, \theta_n;\ \omega_n\right) & l_1 &= g\left(t_n, \omega_n;\ \theta_n\right) \\
k_2 &= f\left(t_n + \Delta t/2, \theta_n + k_1\Delta t/2;\ \omega_n + l_1\Delta t/2\right) & l_2 &= g\left(t_n + \Delta t/2, \omega_n + l_1\Delta t/2;\ \theta_n + k_1\Delta t/2\right) \\
k_3 &= f\left(t_n + \Delta t/2, \theta_n + k_2\Delta t/2;\ \omega_n + l_2\Delta t/2\right) & l_3 &= g\left(t_n + \Delta t/2, \omega_n + l_2\Delta t/2;\ \theta_n + k_2\Delta t/2\right) \\
k_4 &= f\left(t_n + \Delta t, \theta_n + k_3\Delta t;\ \omega_n + l_3\Delta t\right) & l_4 &= g\left(t_n + \Delta t, \omega_n + l_3\Delta t;\ \theta_n + k_3\Delta t\right)
\end{aligned} \tag{20}$$

---

[6] The name semi-implicit comes from the fact that $n+1$ data in the form of ω_{n+1} is being used to compute θ_{n+1}. Also note that like the unmodified Euler method, the Euler–Cromer method is still only a $\mathcal{O}\big(\left(\Delta t\right)^2\big)$ method.

[7] We could also alter the RK4 method to be an implicit method like the Euler–Cromer method, but will not do so here to avoid additional complexity.

III. RESULTS

A. Simulation Methods

We will begin by comparing the results of the two simulation methods, Euler–Cromer and RK4, by looking at plots of $\theta(t)$, $\omega(t)$, and energy versus time. As you can see in Figures 1 through 4, both methods produced virtually identical results for this pendulum. For the energy plots note that we do not expect total energy to be conserved, even at steady state, because F_{Driving} and $F_{\text{Dampening}}$ are external forces that continually doing work on the system. If we turn them off, setting $\alpha_D = 0.0$, $\gamma = 0.0$, we do have energy conservation, see Section IV B.

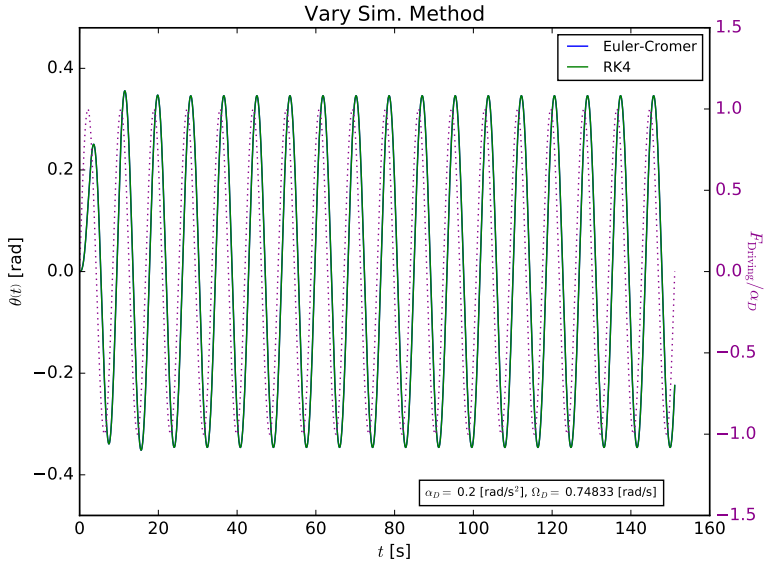

FIG. 1: $\theta(t)$ for the Euler–Cromer and RK4 methods.

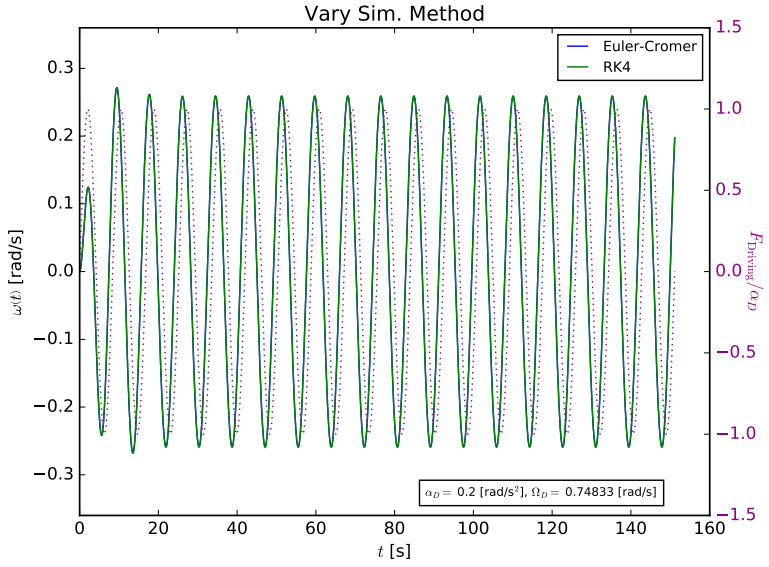

FIG. 2: $\omega(t)$ for the Euler–Cromer and RK4 methods.

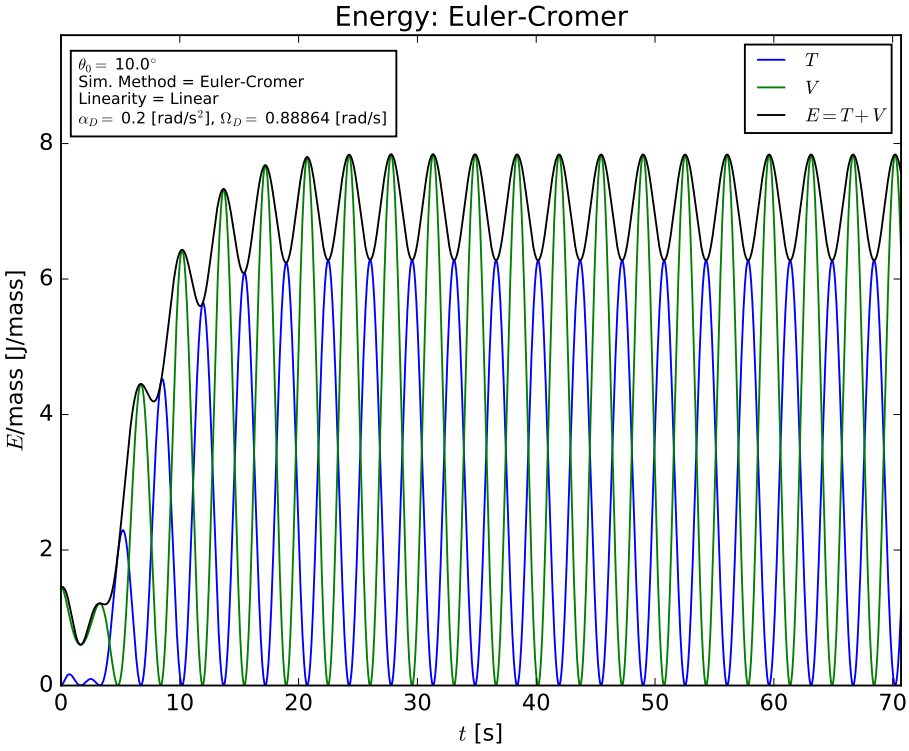

FIG. 3: Kinetic, potential and total energy when using the Euler–Cromer method.

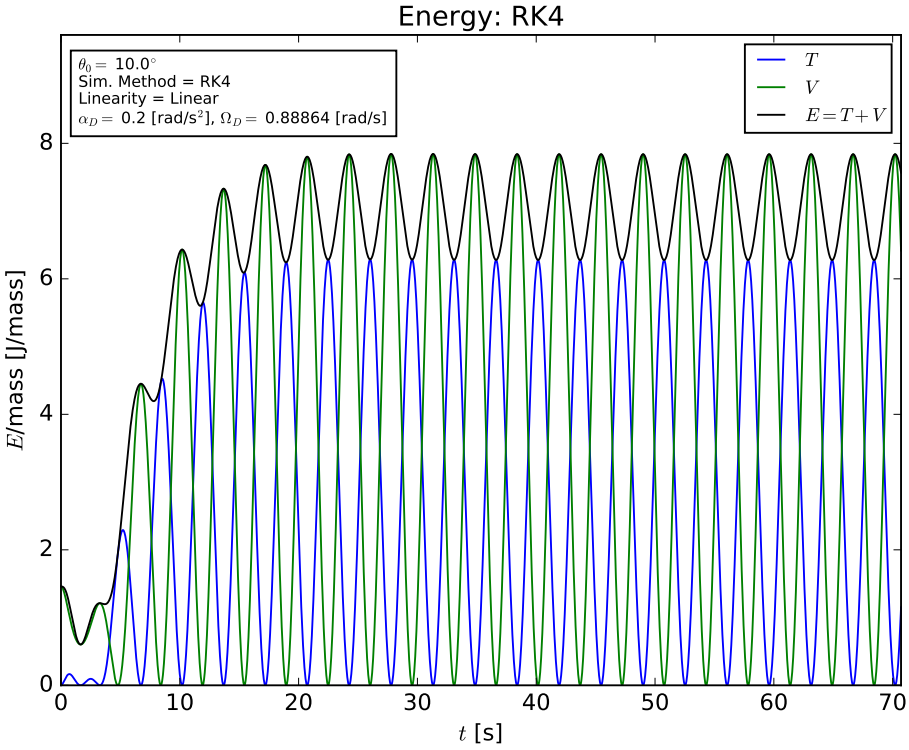

FIG. 4: Kinetic, potential and total energy when using the RK4 method.

B. Resonance

For the rest of the results we will use the RK4 method to simulate the pendulum. By fitting the steady state $\theta(t)$ curve with a sinusoid we are able to extract $\theta_P(\Omega_D)$ and $\phi(\Omega_D)$ for many different value of Ω_D about Ω_{Res}, see Figures 5 and 6. The analysis code was written to automatically perform the fit after waiting a preset number of driving force periods to ensure the steady state had been reached. Supporting plots were made for each Ω_D tested to confirm the fit was good and only included the steady state wave, see Figures 7 and 8 for one example at $\Omega_D = 1.6688$ [rad/s].

The $\theta_P(\Omega_D)$ resonance peak itself was fit twice, to a Gaussian with an offset and to the form of the analytical curve derived earlier (11). As you can see in Figure 5 the analytical "Spectrum Fit" matched the simulation data and the theory curve extremely well, all the fit parameters match to five decimal places. This validates our analytical derivation in Section II, or the numerical simulation code, depending on which you decide to trust more initially. On the other hand, the Gaussian fit was very poor; which is not surprising considering the analytical curve is not symmetric. The chief reason for fitting with a Gaussian is to compare the Full Width at Half Maximum[8] to γ. The Gaussian fit's FWHM was $\approx 4\gamma$ suggesting that γ^2 sets the width of the resonance peak, though this is better seen analytically in (11) as well as in Section IV C.

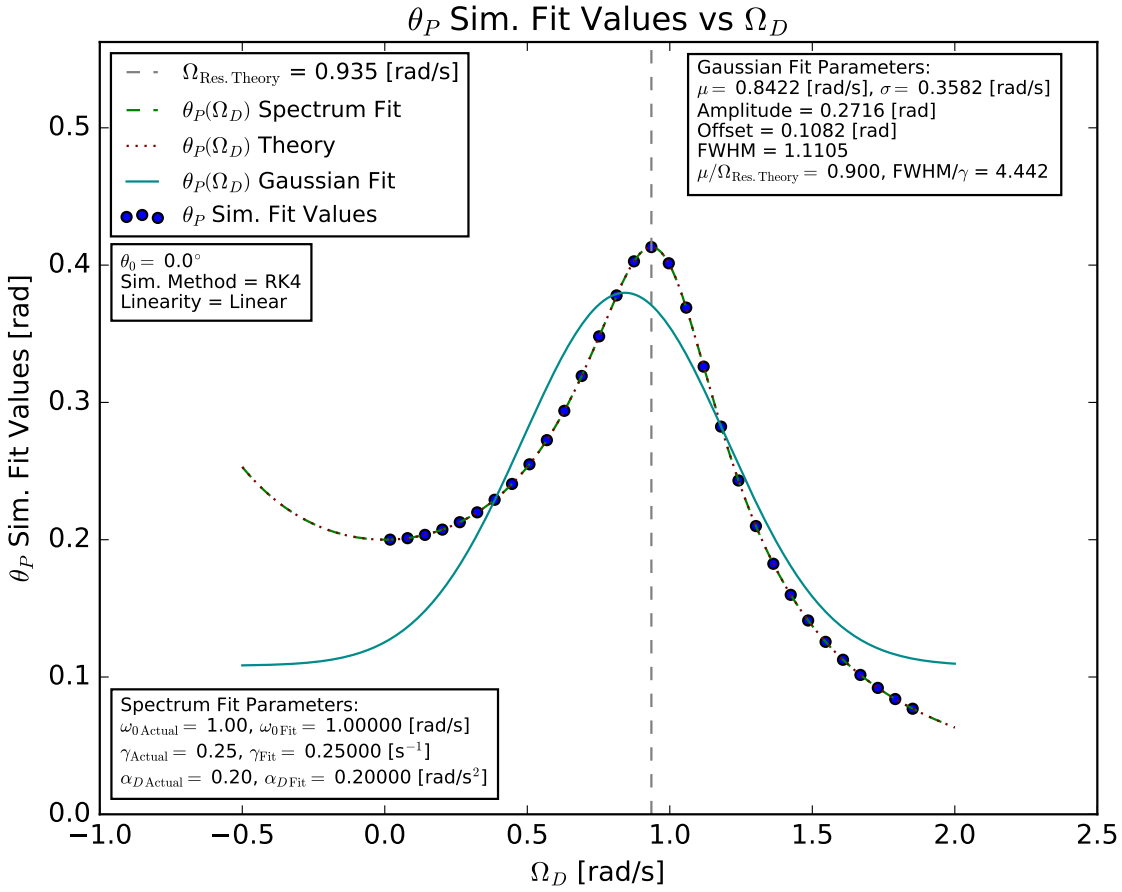

FIG. 5: $\theta_P(\Omega_D)$ resonance curve and fits.

[8] With the offset included, the FWHM $= 2\sigma\sqrt{-2\ln(2^{-1}(1-(\text{offset}/\text{amplitude})))}$, which reduces to the usual FWHM if offset = 0.

The $\phi\,(\Omega_D)$ resonance peak was fit with the analytical curve (12). Again there was very good agreement between the simulation data, the analytical fit curve, and the analytical theory.

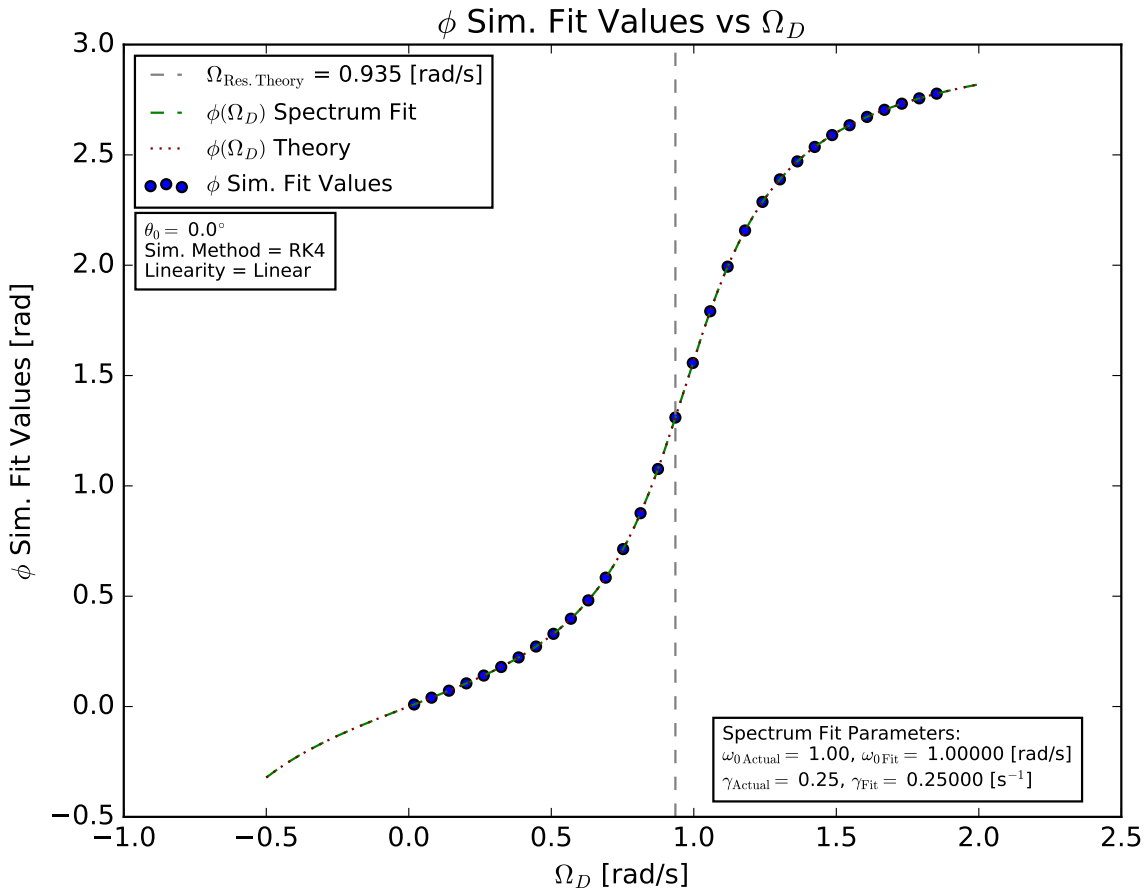

FIG. 6: $\phi\,(\Omega_D)$ resonance curve and fit.

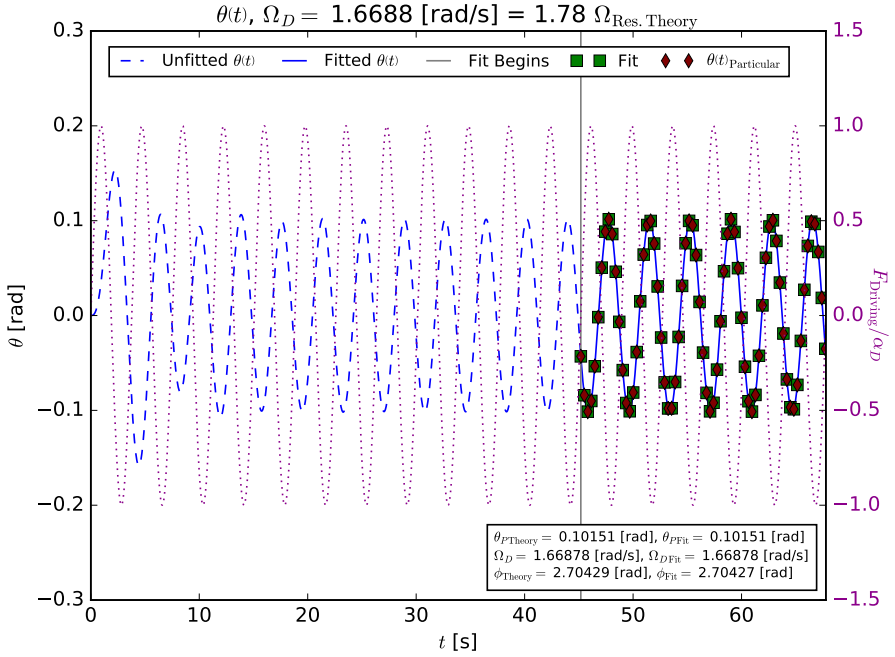

FIG. 7: $\theta\,(t)$ at $\Omega_D = 1.6688$ [rad/s], full view. Note how the fit is performed on data well into the steady state region.

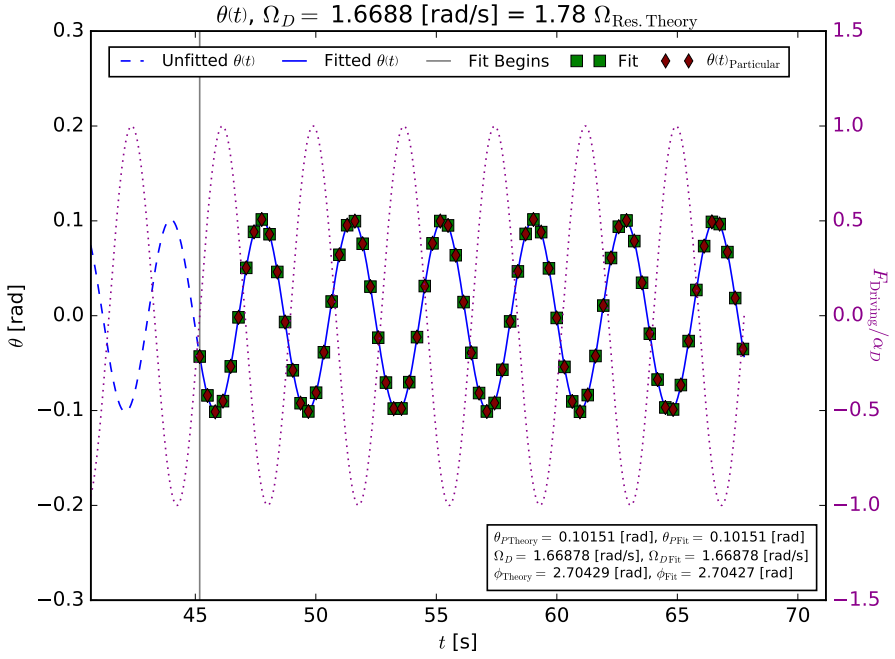

FIG. 8: $\theta\,(t)$ at $\Omega_D = 1.6688$ [rad/s], fit region. The sinusoidal fit typically matched the theory predictions to all the shown decimal places. This Ω_D plot was chosen to be included in particular to illustrate that the data was really being fit – you can see a difference in the last decimal place of the ϕ values.

C. Nonlinear Effects

As we are running a numerical simulation there is no problem in abandoning the small angle approximation and having the restoring force go as $-\omega_0^2 \sin(\theta)$. We only need to change $g(t, \omega;\ \theta)$ to (21) and the Euler–Cromer and RK4 methods will run just as easily as before. This is in sharp contrast to the difficultly of attempting to redo the analytical derivation.

$$g(t, \omega;\ \theta)_{\text{nonlinear}} = -\omega_0^2 \sin(\theta) - 2\gamma\omega + \alpha_D \sin(\Omega_D t) \tag{21}$$

When the driving force amplitude is small, $\alpha_D = 0.2$ [rad/s^2], the pendulum does not move far from $\theta = 0$. In this case we expect the small angle approximation hold, and indeed there are no real differences between the linear and nonlinear simulations, see Figures 9 and 10. However, when the driving force is increased, $\alpha_D = 1.2$ [rad/s^2], it drives the pendulum up to higher θ's, breaking the small angle approximation. In this case significant deviations occur between the linear and nonlinear simulations, see Figures 11 and 12. The nonlinear simulation is the correct method to use here.

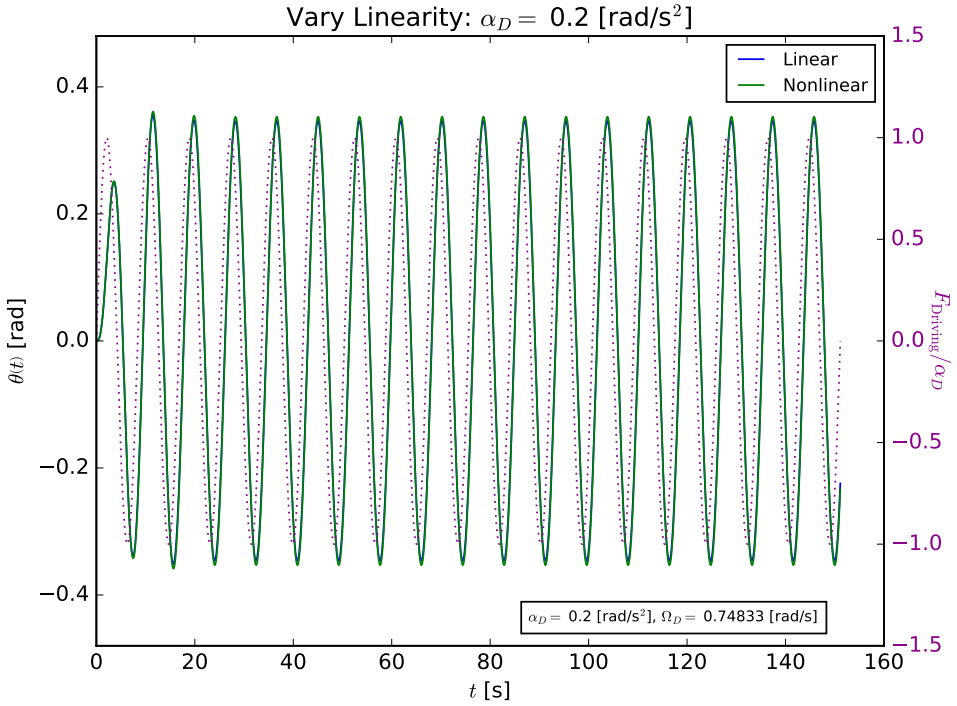

FIG. 9: $\theta\,(t)$ for the linear and nonlinear restoring force, $\alpha_D = 0.2$ [rad/s^2].

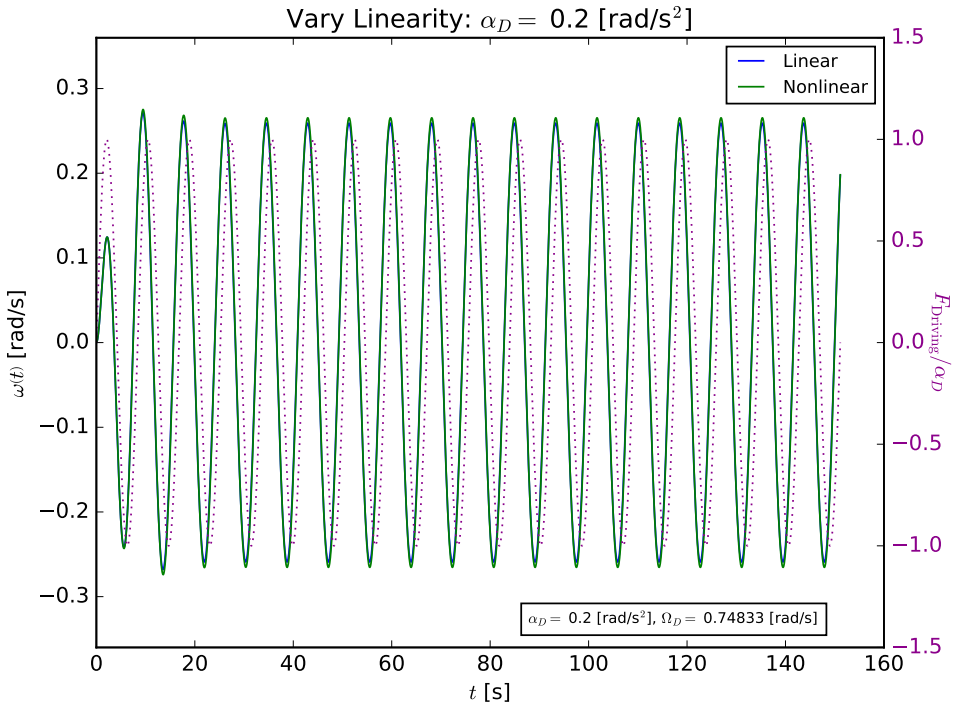

FIG. 10: $\omega\,(t)$ for the linear and nonlinear restoring force, $\alpha_D = 0.2$ [rad/s^2].

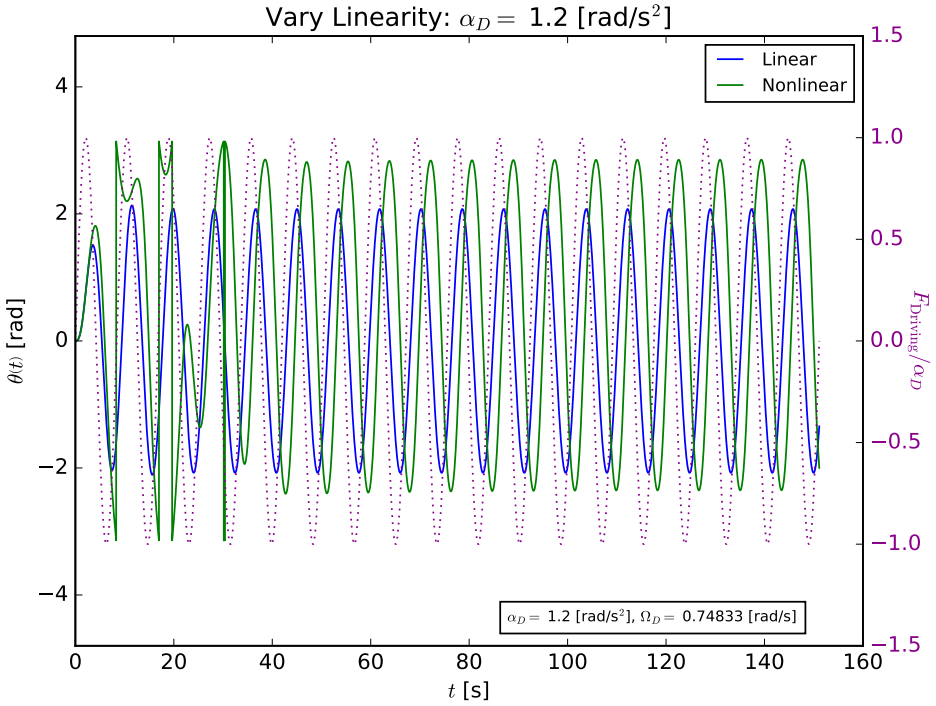

FIG. 11: $\theta\,(t)$ for the linear and nonlinear restoring force, $\alpha_D = 1.2$ [rad/s^2].

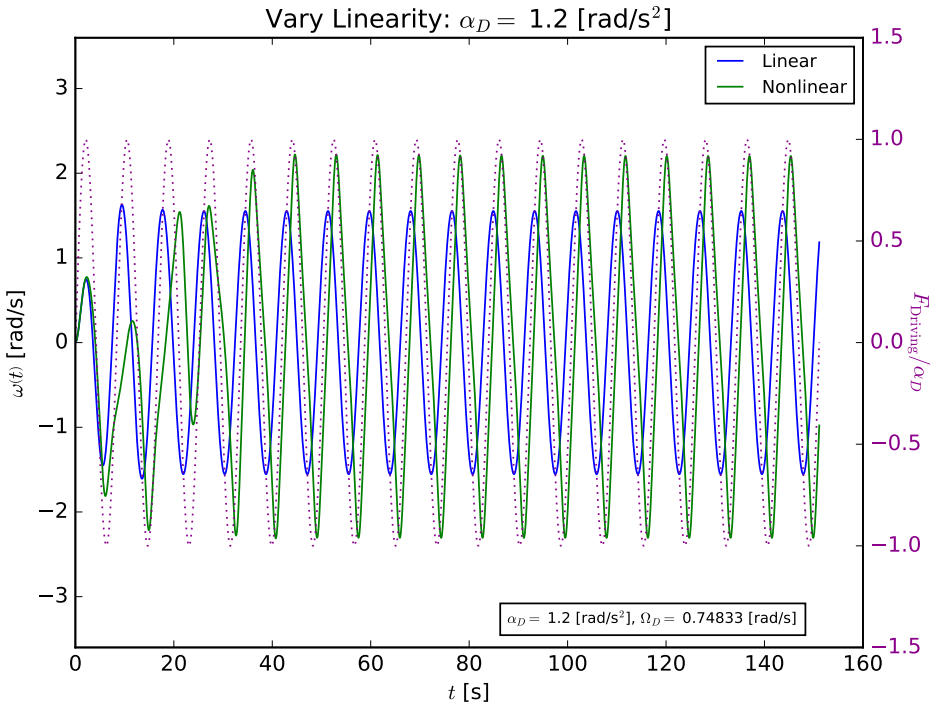

FIG. 12: $\omega\,(t)$ for the linear and nonlinear restoring force, $\alpha_D = 1.2$ [rad/s^2].

D. Chaos and Lyapunov Exponents

When working through the theory of the linear pendulum we showed that the initial conditions only affected the transient solution which decayed away exponentially to leave the steady state sinusoid. As such two different pendulums, or systems, with slightly different initial conditions are expected to converge over time. However if we force the pendulum to behave nonlinearly, by increasing α_D or θ_0 till the small angle approximation breaks down, we must use $-\omega_0^2 \sin(\theta)$ as the restoring force and can no longer rely on the linear theory. Now if two nonlinear systems are setup with very slightly different initial conditions they may no longer converge, but could instead diverge, even exponentially diverge, over time[9]. Systems displaying such exponential divergence for small changes in initial conditions are classified as chaotic and can be quantitatively described by a Lyapunov Exponent λ, defined in (22) where $|\Delta\theta(t)|$ is the difference in position[10] between the systems at time t and $|\Delta\theta_0|$ is the difference in initial position.

$$\left|\Delta\theta(t)\right| = \left|\Delta\theta_0\right| e^{\lambda t} \tag{22}$$

While any combination of initial conditions can be altered to produce chaotic behavior, we will only be changing θ_0 itself by $0.001 \leq \Delta\theta_0 \leq 0.005$ [rad/s] in our simulation. The resulting $|\Delta\theta(t)|$ values are so small we instead plot $\ln(|\Delta\theta(t)/\Delta\theta_0|)$ which also helps by linearizing the data. To find λ we then fit the linearized plot with (23)[11] over the region in time where the systems are exponentially diverging.

$$\ln\left(\left|\frac{\Delta\theta(t)}{\Delta\theta_0}\right|\right) = c_{\text{Fit}} + \lambda_{\text{Fit}} t \tag{23}$$

By repeating the simulation and fit multiple times for small changes in $\Delta\theta_0$ we can average the λ_{Fit}'s and come up with an estimate of λ of the system. Three different driving force amplitudes where considered in turn, $\alpha_D = 0.2$, 0.5, and 1.2 [rad/s^2]. The first two where small enough that the system behaved linearly and did not exhibit chaos, indeed the λ_{Fit}'s < 0 verified the transient solution's exponential decay, see Figures 13–16.

For $\alpha_D = 1.2$ [rad/s^2], previously looked at in Section III C, the system was again nonlinear and showed chaotic behavior, see Figure 17. The mean λ_{Fit} was found to be 0.1251 [s^{-1}], although the structure in Figure 18 shows that the mean alone may not adequately describe the situation. For the purposes of this work we will leave it here, though individuals interested in the particulars of system itself could characterize this behavior further.

---

[9] Each system is still fully deterministic once the initial conditions are specified. Chaotic system are just extremely sensitive to the initial conditions

[10] In general we can look at the difference in phase space, but position is fine here.

[11] An offset c is included so the fit is not overly constrained, even though c should ideally be 0 as we have already divided by $\Delta\theta_0$.

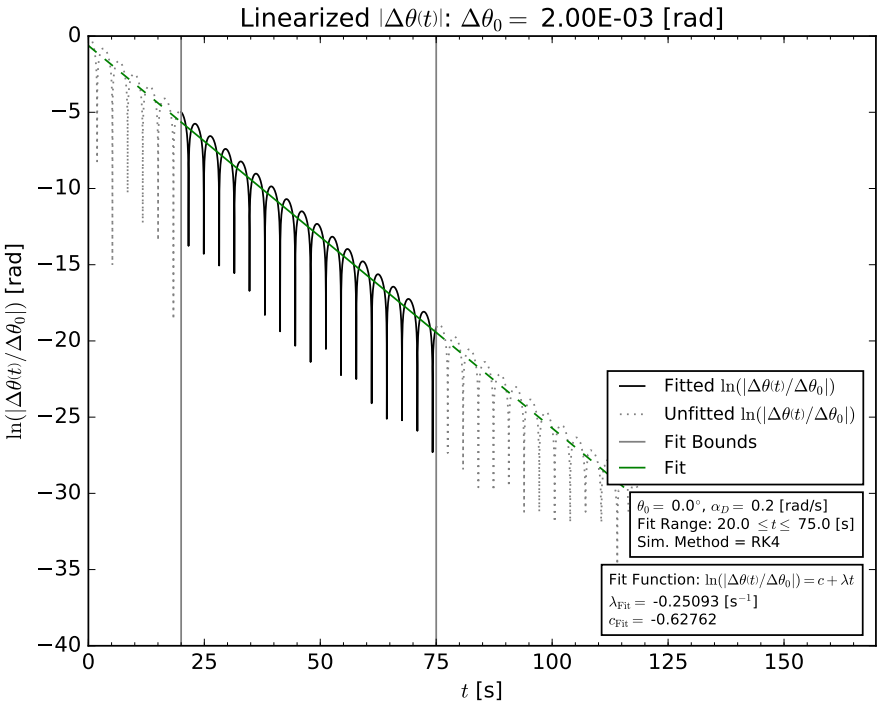

FIG. 13: $\left|\Delta\theta\left(t\right)\right|$ curve and linear fit, $\alpha_D = 0.2$ [rad/s^2], nonchaotic regime.

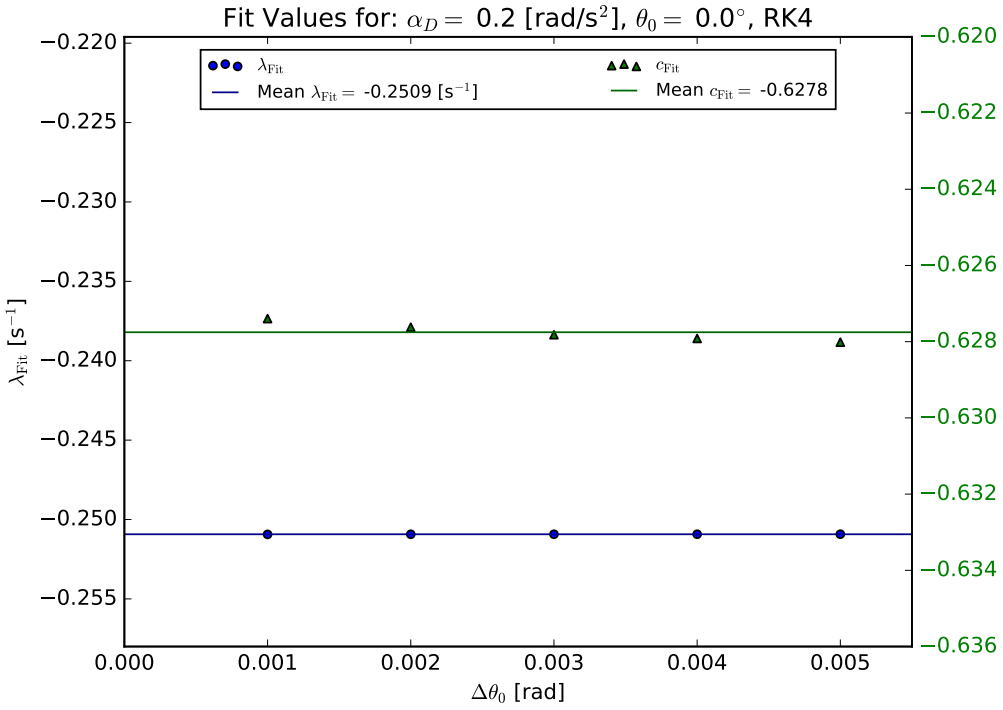

FIG. 14: λ_{Fit} curve and mean, $\alpha_D = 0.2$ [rad/s^2], nonchaotic regime.

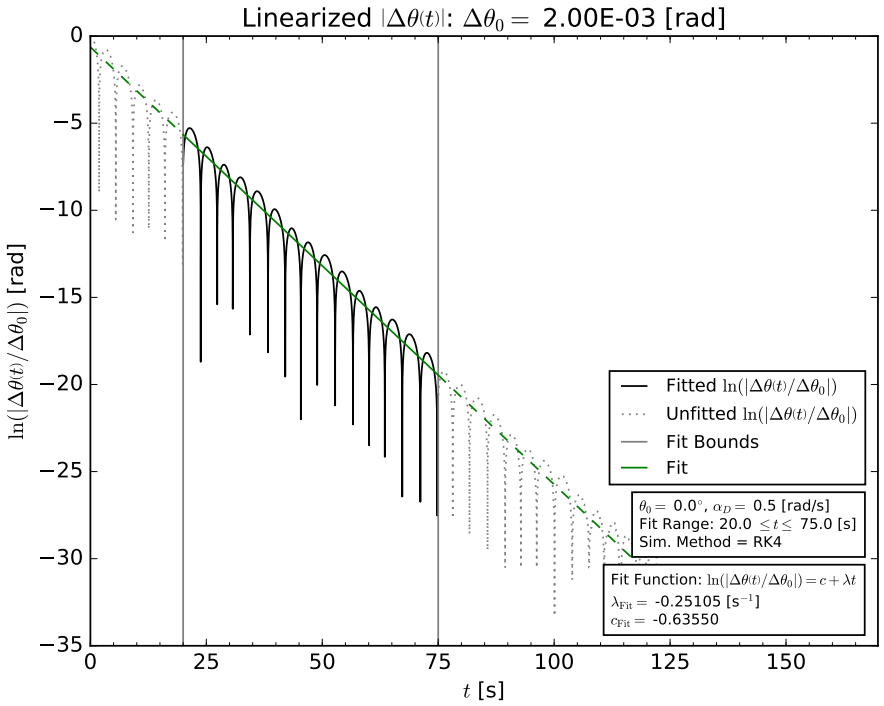

FIG. 15: $\left|\Delta\theta\left(t\right)\right|$ curve and linear fit, $\alpha_D = 0.5$ [rad/s^2], nonchaotic regime.

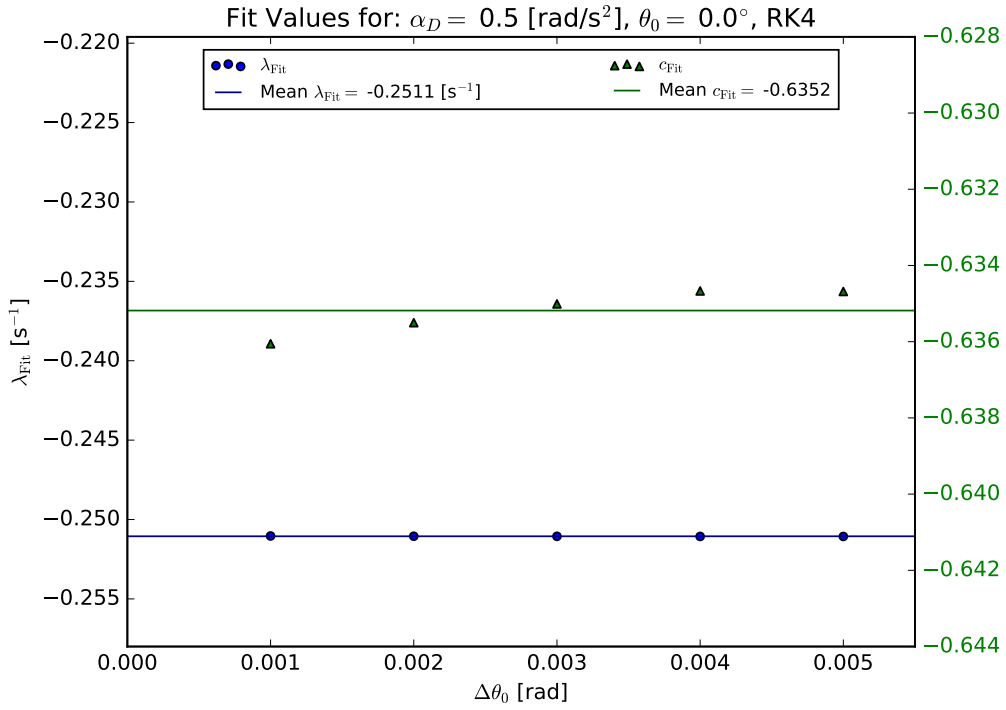

FIG. 16: λ_{Fit} curve and mean, $\alpha_D = 0.5$ [rad/s^2], nonchaotic regime.

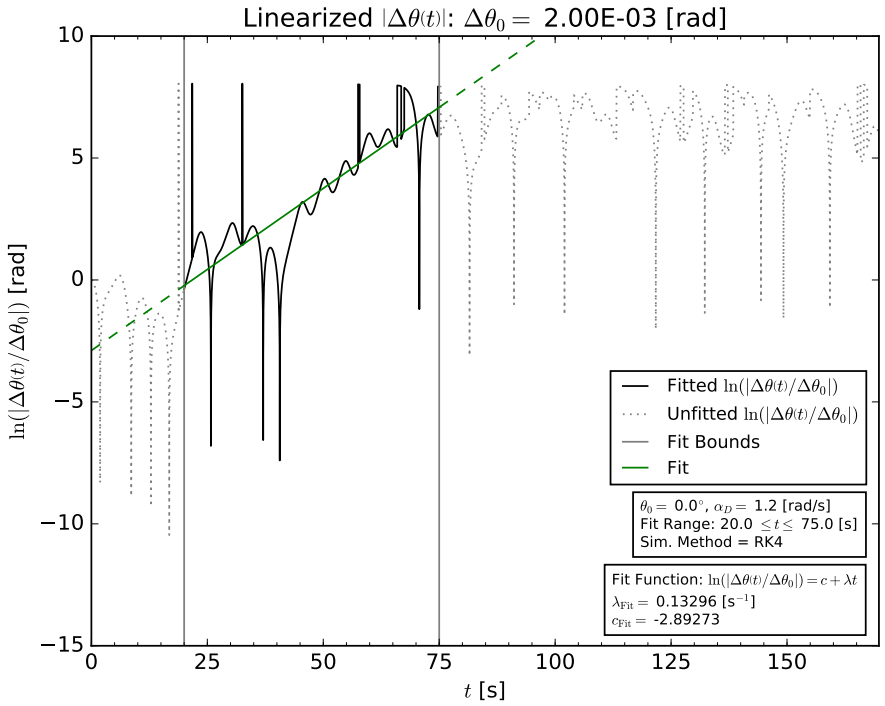

FIG. 17: $\left|\Delta\theta\left(t\right)\right|$ curve and linear fit, $\alpha_D = 1.2$ [rad/s^2], chaotic regime.

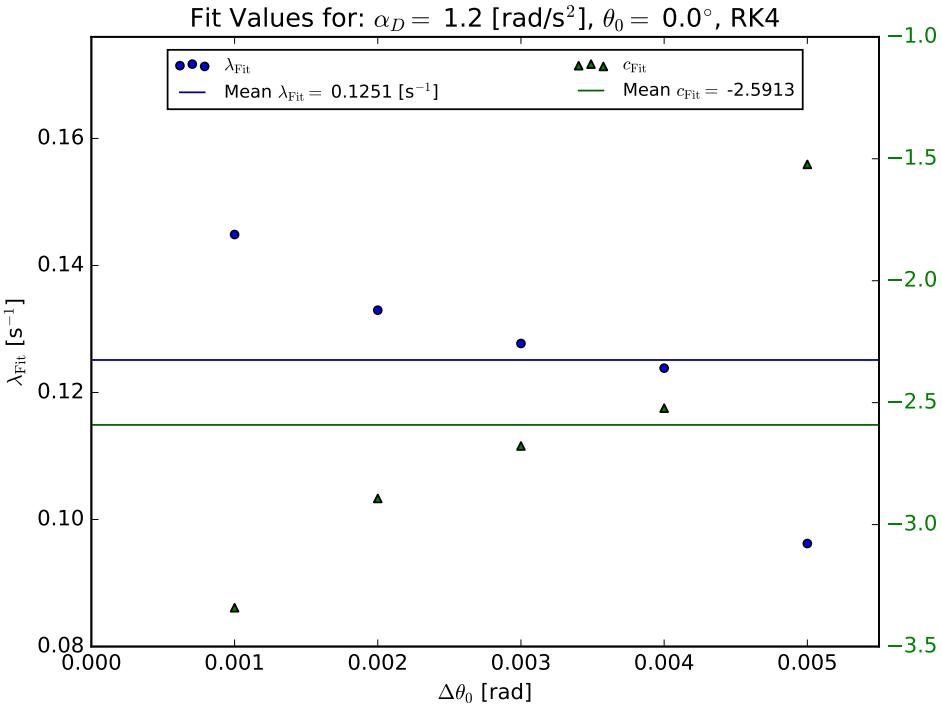

FIG. 18: λ_{Fit} curve and mean, $\alpha_D = 1.2$ [rad/s^2], chaotic regime.

IV. EXTRA MATERIAL

A. Nonlinear Resonance Curves

Since the simulation code is already written we can also see what the nonlinear restoring force does to the resonance curves, Figures 22 and 23. For this resonance sweep α_D was left at 1.2 [rad/s^2] while θ_0 was increased to 45° to make the pendulum as nonlinear as possible. Note that the theory curves are still using the linear, small angle approximation out of necessity, but this is fine as it allows us to see how far the resonance curves diverge from the linear theory. With these parameters the pendulum exhibits very interesting behavior; alternating between high and low frequency beats at low driving frequencies, Figure 19, periodically swinging over the top at intermediate driving frequencies, Figure 20, and behaving somewhat linear at high driving frequencies, Figure 21.

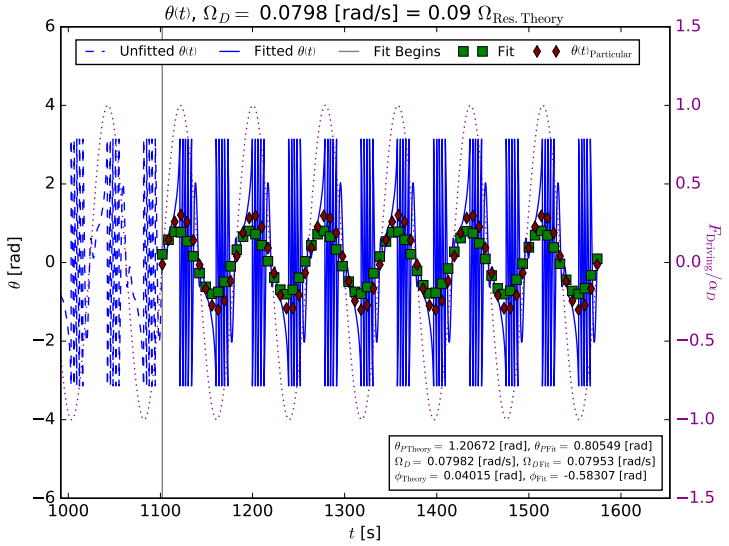

FIG. 19: Nonlinear $\theta\,(t)$ at low $\Omega_D = 0.0798$ [rad/s].

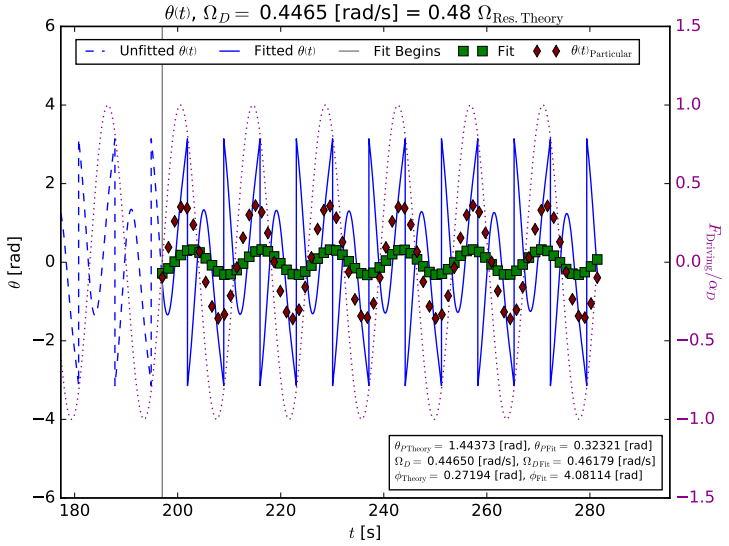

FIG. 20: Nonlinear $\theta\,(t)$ at intermediate $\Omega_D = 0.4465$ [rad/s].

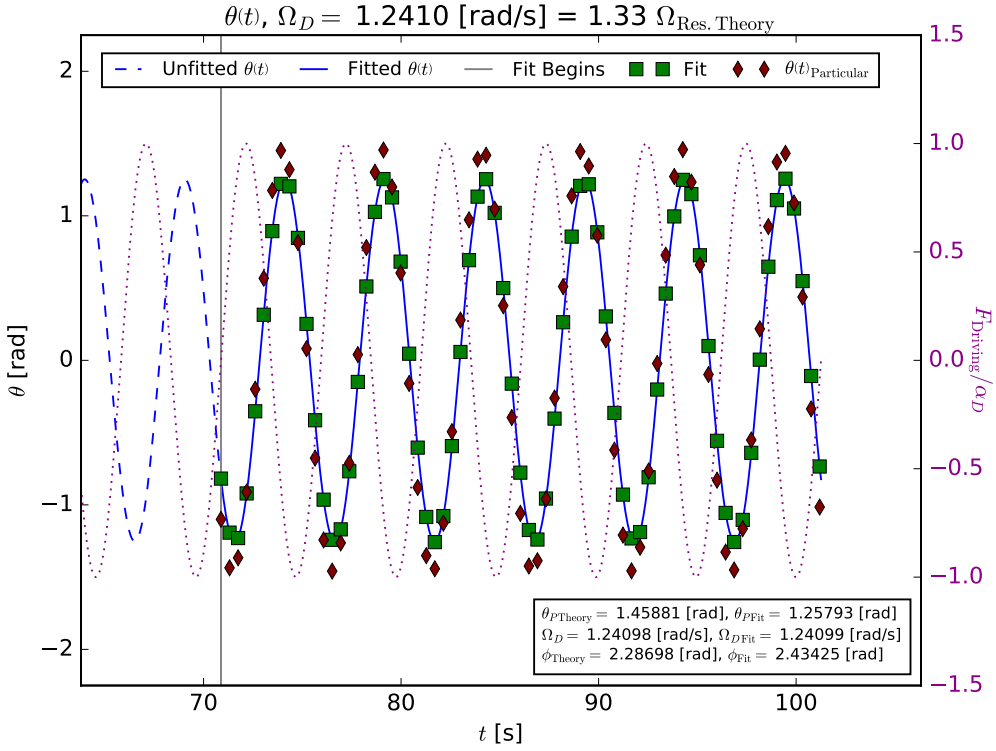

FIG. 21: Nonlinear $\theta\,(t)$ at high $\Omega_D = 1.2410$ [rad/s].

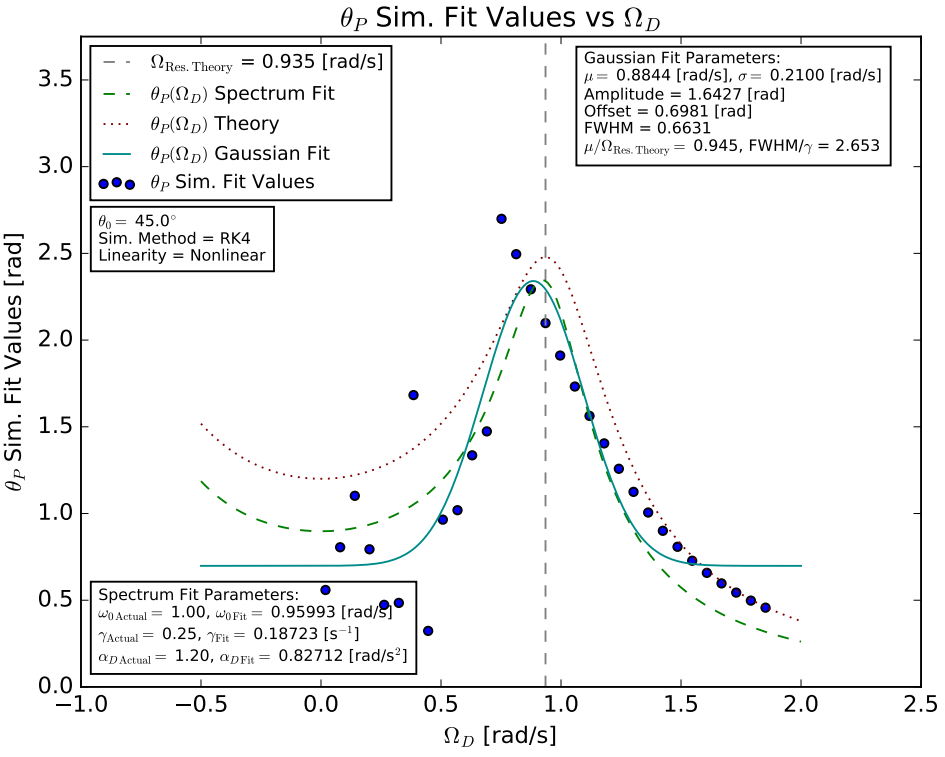

FIG. 22: $\theta_P\,(\Omega_D)$ resonance curve and fits, nonlinear restoring force. Points at low to intermediate Ω_D should be disregarded as the sinusoidal fits are clearly non–convergent there.

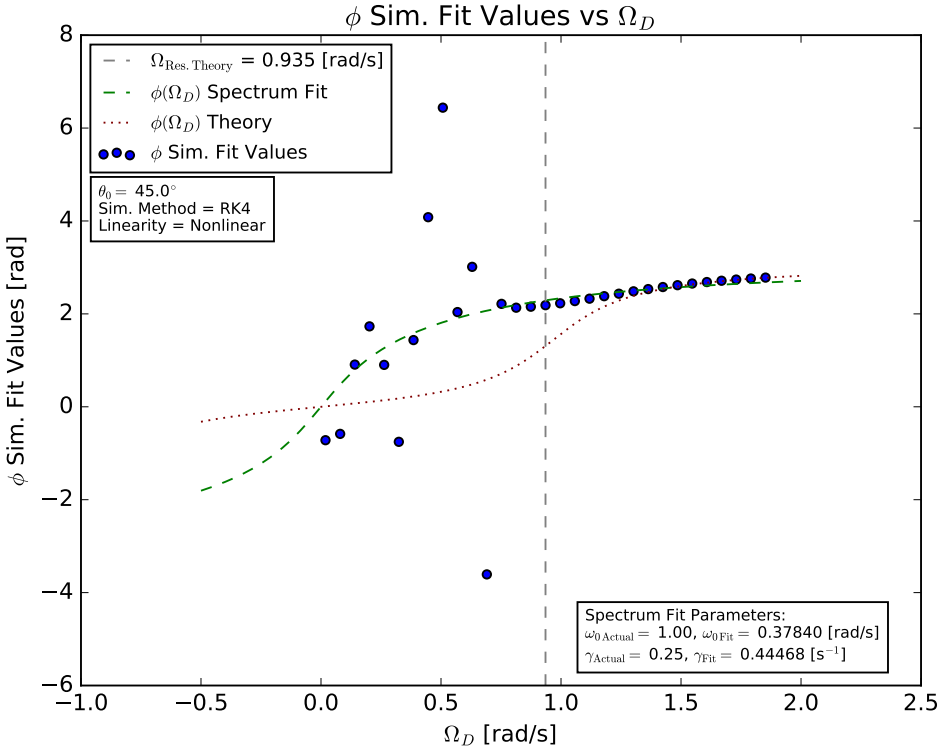

FIG. 23: $\phi\,(\Omega_D)$ resonance curve and fit, nonlinear restoring force. Points at low to intermediate Ω_D should be disregarded as the sinusoidal fits are clearly non–convergent there.

B. Energy Conservation

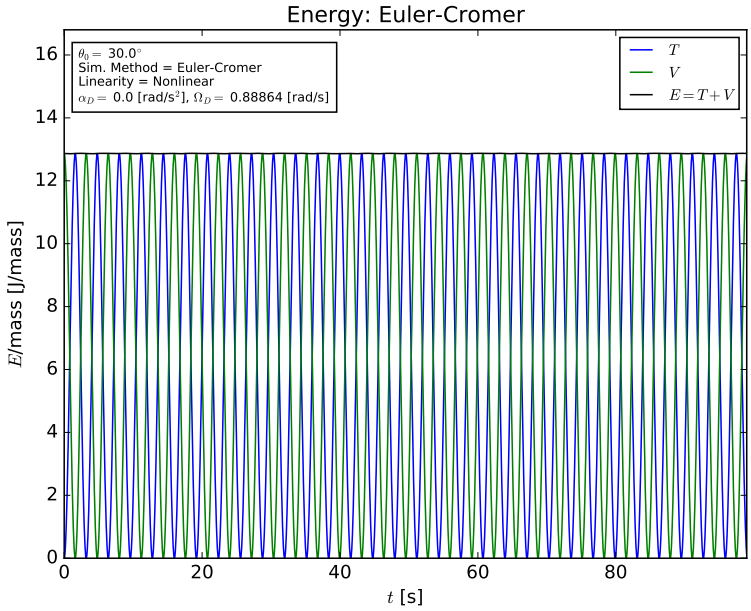

FIG. 24: Free pendulum, $\alpha_D = 0.0$, $\gamma = 0.0$: Kinetic, potential and total energy when using the Euler–Cromer method.

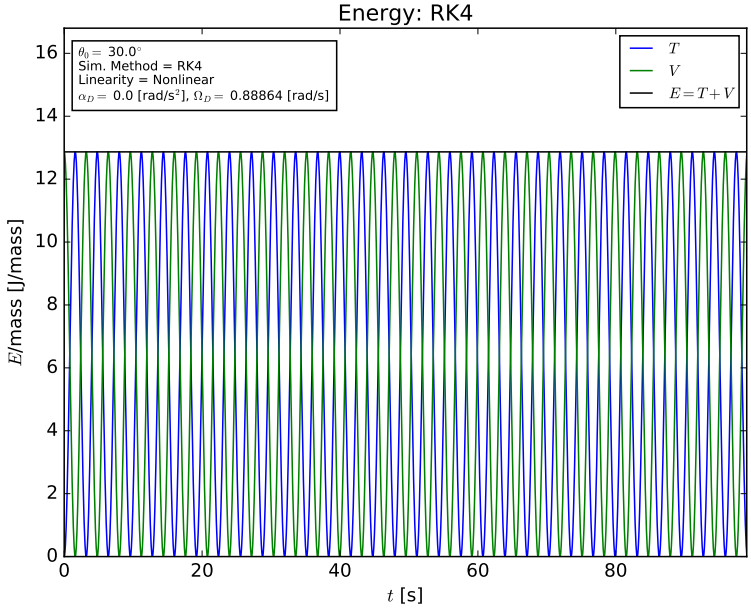

FIG. 25: Free pendulum, $\alpha_D = 0.0$, $\gamma = 0.0$: Kinetic, potential and total energy when using the RK4 method.

C. Analytical Resonance Curves

θ_P Analytical_Resonance_Spectrum

In[30]:=
```
Clear["Global`*"]
```

In[31]:=
```
thetaP[gamma_, Omega_] := ((1 - Omega^2)^2 + 4 gamma^2 Omega^2)^-0.5;
```

In[32]:=
```
gamma = 0.25;
p1 = Plot[thetaP[gamma, Omega], {Omega, 0, 2}, PlotStyle → Blue];
```

In[34]:=
```
gamma = 0.5;
p2 = Plot[thetaP[gamma, Omega], {Omega, 0, 2}, PlotStyle → Green];
```

In[36]:=
```
gamma = 1;
p3 = Plot[thetaP[gamma, Omega], {Omega, 0, 2}, PlotStyle → Cyan];
```

In[38]:=
```
Show[p1, p2, p3, AxesLabel → {"Ω_P[rad/s]", "θ_P"}]
```

Out[38]=